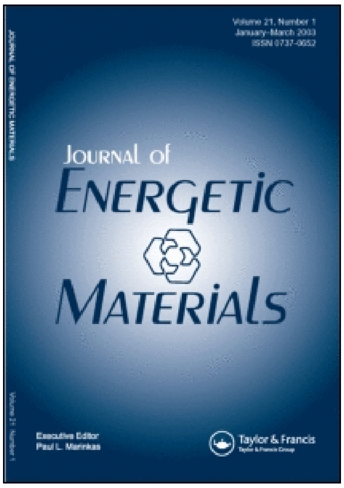

Journal of Energetic Materials
Publication details, including instructions for authors and subscription information:
http://www.informaworld.com/smpp/title~content=t713770432

Real-time analysis of hns detonation products: Carbon clusters

Normand C. Blais[a]
[a] Chemistry Division, Los Alamos National Laboratory, Los Alamos, NM

To cite this Article Blais, Normand C.(1987) 'Real-time analysis of hns detonation products: Carbon clusters', Journal of Energetic Materials, 5: 1, 57 — 76

To link to this Article: DOI: 10.1080/07370658708012349

URL: http://dx.doi.org/10.1080/07370658708012349

REAL-TIME ANALYSIS OF HNS DETONATION PRODUCTS: CARBON CLUSTERS

Normand C. Blais
Los Alamos National Laboratory
Chemistry Division, MS G738
Los Alamos, NM 87545

ABSTRACT

We have determined the mass spectrum and the time evolution of the freely expanding products of HNS detonation. The products arriving at the detector earliest have velocities of 8 km s^{-1}; except for hydrogen, this is characteristic of all of the products irrespective of mass. The spectrum is dominated in intensity by products at mass 28, which we ascribe as composed of 80% CO and 20% N_2. These account for nearly half the total products. The remaining products are spread over many mass peaks from mass 12 to mass 60, the most important being H_2, N_2O, CO_2 and carbon clusters. We observe carbon in clusters, C_n, with $1 \leq n \leq 5$ in a distribution that decreases monotonically with n. Carbon cluster distributions are also obtained under conditions of partial confinement by solid Xe at 30 K and the distributions are found to be relatively unchanged. We compare our mass spectrum with those obtained under conditions closer to equilibrium and to earlier measurements of the same kind with PETN.

Journal of Energetic Materials vol. 5, 57-76 (1987)

Published in 1987 by Dowden, Brodman & Devine, Inc.

INTRODUCTION

We present the results of measuring the mass spectrum of the freely expanding products from laboratory scale detonations of hexanitrostilbene, HNS. We are interested in examining this explosive because one of its major constituent products is soot,[1] or solid carbon. The study promises to make an interesting contrast with another explosive for which we've reported similar measurements,[2] pentaerythritol tetranitrate, PETN. Both HNS and PETN are characterized as high explosives, but HNS ($C_{14}H_6N_6O_{12}$) is oxygen poor compared to PETN ($C_5H_8N_4O_{12}$) in the ratio of oxygen atoms to carbon atoms. The resulting immediate detonation products have a different product spectrum, especially in the formation of carbon molecules in HNS that ultimately become soot. The energy release by forming soot is a significant part of the detonation energy,[3] sometimes making the difference between predicting the overall reaction as even being exoergic or endoergic.

The kind of measurements that we make allows us to detect many radicals and reaction intermediates that are not observed using other methods. Our previous work suggests that those products that arrived early on the time scale of our experiments originated from layers of the explosive nearest the detector.[2] While these molecules have experienced many collisions in the expansion process, there were far fewer than the number suffered by products originating deeper in the bulk of the explosive. These early arriving molecules therefore have a mass and energy spectrum that depart considerably from the equilibrium conditions that would result from measurements taking longer times and having more constrained expansion conditions. The carbon molecule distributions we present here are thus an indication of the distribution of carbon species closely following detonation.

The problem of soot formation is a long standing one that is familiar to those studying high temperature gas-phase combustion of hydrocarbons.[4] Carbon clusters are thought to play an important part in this process, but the mechanism by which soot results from carbon bearing molecules is still not well understood. Small clusters, such as C_2, C_3, C_2H are easily observed in large amounts in flames that are luminous from large carbon clusters.[5] Perhaps by undertaking analogous measurements to those done in combustion studies, the kind that we are reporting, we can add to the information about the mechanism of soot formation. There is evidence that the chemical reactions that drive the detonation wave in a high explosive do not have the bimolecular characteristic of gas-phase reactions, but clearly those reactions that occur during the product expansion are describable as gas phase. We hope to be able to distinguish in which phase soot is formed by measuring the distribution of the carbon clusters in the detonation. The distributions we obtain, as we will see below, are unlike those obtained from the newly developed laser ablation methods of forming carbon clusters.[6] Our distributions contain much smaller clusters, such as are found in flames.

EXPERIMENTAL

The apparatus used for these studies was described in detail earlier.[2] Briefly, 22-mg pellets of HNS (PANTEX 4307-07-MDT-01) having a density of 1.55 to 1.60 are detonated electrically in a large vacuum chamber. The dimensions of the chamber are such that the expanding products of the detonation reach collisionless molecular flow and enter the detector before they can collide with either ambient molecules or with product molecules that have had a wall collision. The time and intensity distribution of a particular mass are measured using a quadrupole mass filter located in an ultrahigh vacuum chamber isolated by apertures from the detonation chamber. For each mass measured a pellet must be detonated.

For one aspect of the reported work, we modified the apparatus so that the carousel supporting the pellet and detonators could be cooled to 30 K. With this modification, we could deposit an overlayer of solid Xe onto the HNS pellet. This allowed us to change the expansion environment of the products to observe any changes in the carbon cluster distribution. This apparatus modification has also been described elsewhere.[7]

Molecular velocity distributions are obtained by time-of-flight measured over a distance of 110 cm.

RESULTS

Figure 1 is a plot of the raw data as it is collected in the multichannel scaler (MCS) for two masses M = 15 and M = 44. The dwell time, Δt, for collection is 10 μs in each channel. The transit time from pellet to detector is taken to be the time at the center of each n'th channel:

$$t = (n - 1/2)\Delta t$$

Figure 2 is a mass spectrum for HNS. We obtained it by summing all of the counts above background for each mass indicated, stopping at channel 40 so that the maximum arrival time considered is about 400 μs. We did this because several of the time distributions showed a subsequent rise in intensity after channel 40, as shown in Fig. 1, for which we couldn't account. Fearing that these molecules were not direct products of detonation but had been "reshocked" by collisions with the detonator supports of our apparatus, we chose to exclude them from the counting procedures. Thus, we are restricting our data to the early arriving molecules, those that are closest to being the detonation products. By so doing, we also avoid the necessity of converting each time density distribution to a time flux distribution to construct Fig. 2. Each mass had a remarkably similar time distribution up to channel 40 so that the conversion from density to flux would not alter the intensities within the uncertainties of our measurements.

As we will discuss later, the mass peaks for Fig. 2 were corrected for ionization efficiency[8] and mass transmission of the quadrupole mass filter.

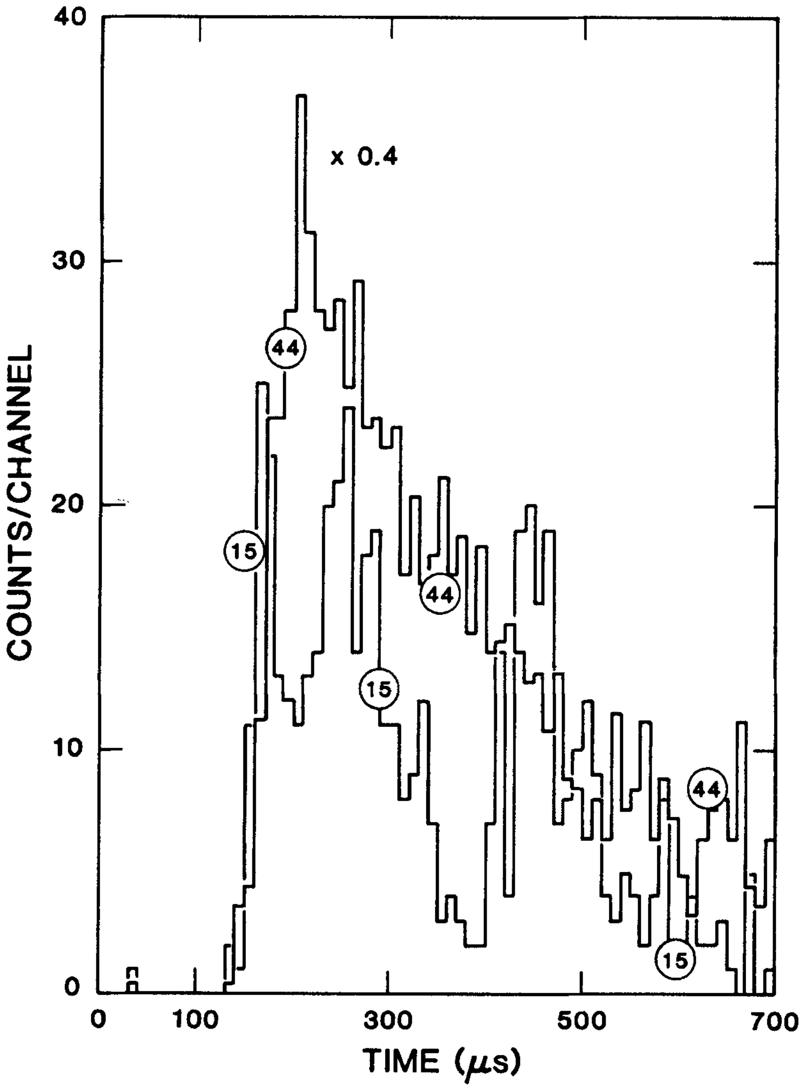

FIGURE 1
Detonation product time of arrival distributions. The counts stored in each channel of a multichannel scaler are plotted as a function of time after detonation for two masses, M=15 and M=44. The flight path is 110 cm.

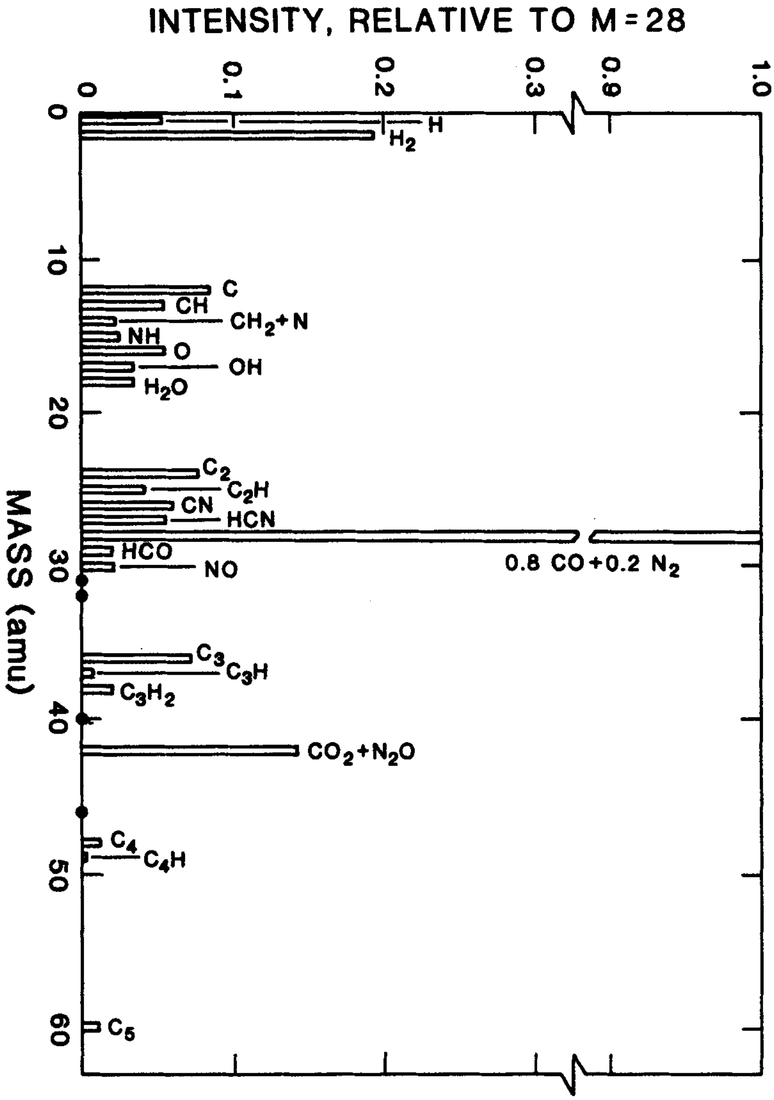

FIGURE 2
Mass spectrum of HNS detonation products. The intensities are relative to M=28, which is given unit intensity. Species were assigned to each mass as described in the text. Dots indicate masses at which measurements were made but no products were detected. Selected measurements were made to M=720, but no signals were obtained.

Besides searching for products at masses larger than those shown in Fig. 2 (up to M = 402), we also paid particular attention to masses that correspond to large clusters of carbon up to C_{60}, M = 720. The only signals that were clearly evident above electrical noise were those up to C_5, M = 60. In addition to being plotted in Fig. 2, we've plotted them separately in Fig. 3 in a different way, as relative ratios of cluster intensity. Also, we include the distribution for carbon cluster formation under very different detonation conditions.

For the distribution shown in open triangles, we detonated the HNS pellets at low temperatures, 30 K, and covered the surface of each pellet with 20 to 30 mg of Xe condensed on the surface as a solid. This layer approximated an inert layer of HNS equal to the mass of the pellet, so that the carbon arriving at the detector was now equivalent to carbon formed near the center of the pellet for an unconfined detonation. Our intent was to see if larger clusters of carbon were formed under more confined conditions, or if the distribution in cluster size was changed markedly by the confinement. Figure 4 shows a time distribution in carbon clusters taken under ordinary conditions, and although the effect is not large and the shot-to-shot reproducibility is not good, it seemed to us that the larger carbon clusters always arrived at the detector a little later than C_1 or C_2, indicating that they were formed deeper in the expanding gases. Our anticipation of larger clusters appearing under confinement was not borne out. As Fig. 3

shows, there is no drastic difference between the two conditions of detonation. In fact, the relative prominence of C_1 is increased by confining the detonation. Incidentally, we saw no differences between the carbon distributions when the pellet was cold or when it was at room temperature, so long as the Xe overlayer was absent.

DISCUSSION

As we found was the case for our earlier work on PETN, the arrival time at threshold for all of the molecules was the same almost irrespective of mass. This time was about 135 μs corresponding to a velocity of 8 km s^{-1}, somewhat lower than the 11 km s^{-1} found for PETN. Both hydrogen, M = 1 and M = 2 arrived slightly earlier, with velocities about 9 km s^{-1}, indicating that these earlier arriving molecules were not fragments from heavier molecules produced in the ionizer detector. For those molecules in the time region of 400 μs that we include in our analysis, the velocities are determined by the hydrodynamic expansion of the product gases. It is as if the molecules came from a free-jet expansion of a mixture of gases in which there is very little "slippage" between the components of the mixture.

In assigning the mass peaks to Fig. 2 we were guided by the necessity to maintain the correct mass balance to the system. We guessed at what species constituted the principal constituent of each peak, and corrected the intensity for its mass transmission

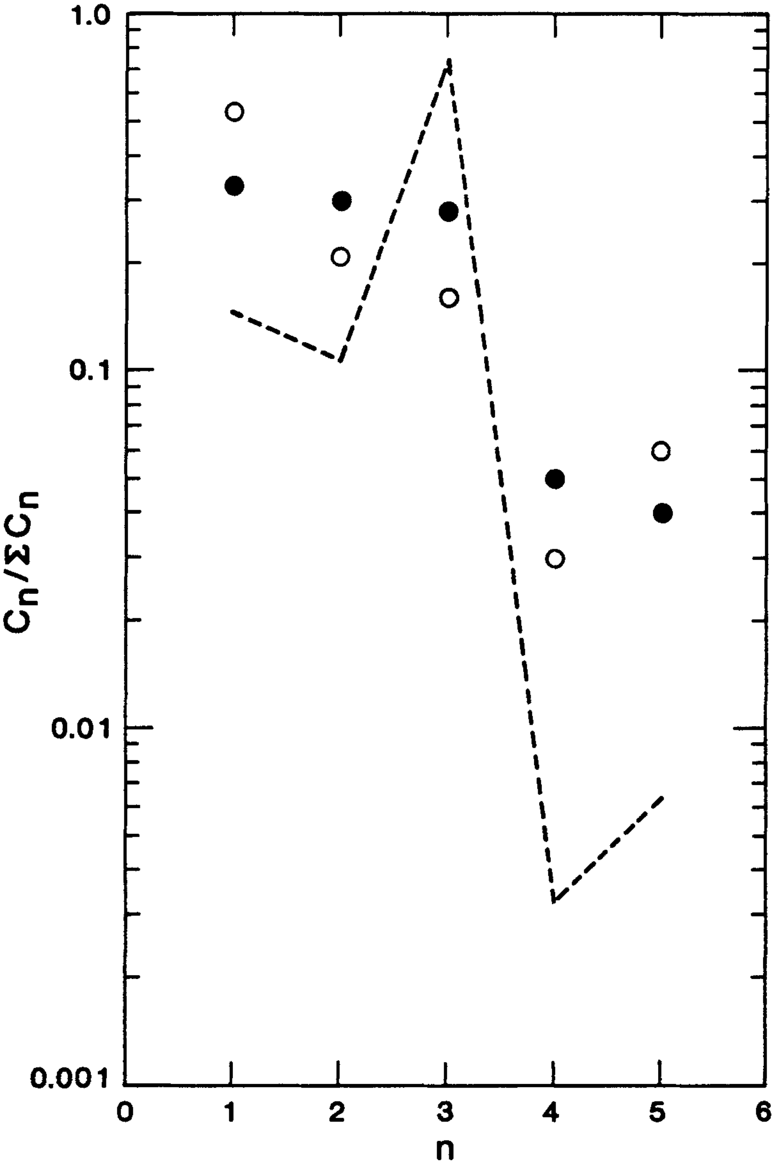

FIGURE 3
Carbon cluster intensity distribution from HNS detonations. The relative intensity of a cluster containing n carbon atoms is shown under two different detonation conditions. The closed circles are for room temperature, unconfined detonations. The open circles are detonations at 30 K with an overlayer of solid Xe covering the HNS pellet. The dashed line is an equilibrium distribution of carbon clusters at 3400 K and 0.01 bar carbon partial pressure.

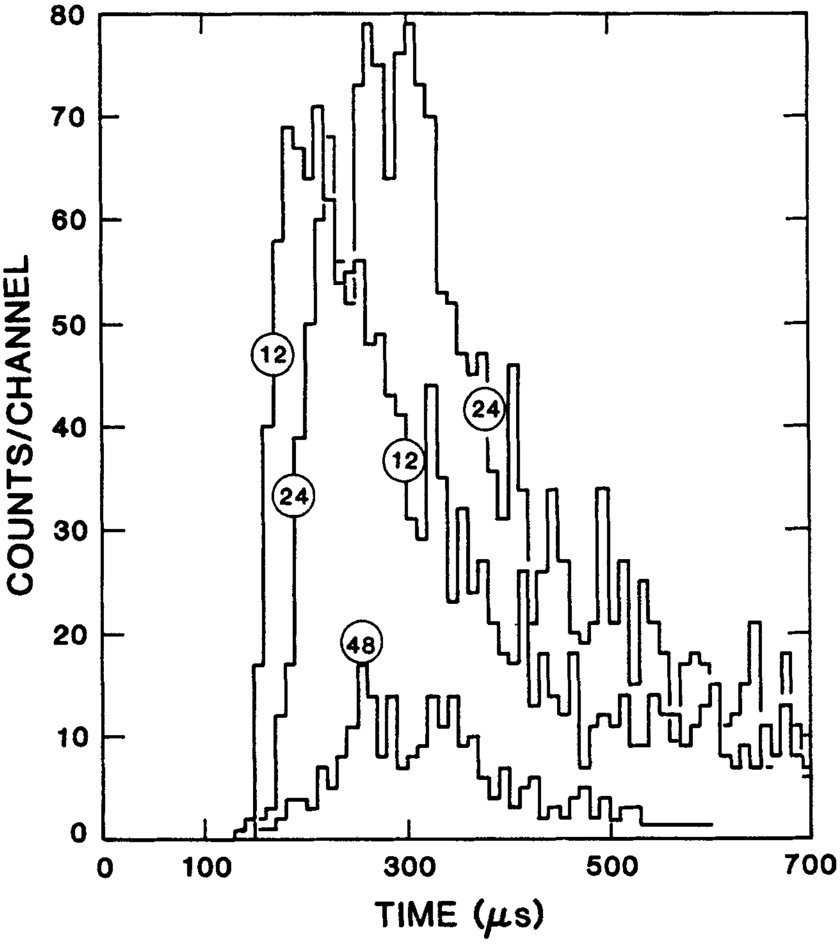

FIGURE 4
Carbon cluster time of arrival distribution. These are similar to Fig. 1, but for three clusters of carbon containing 1, 2, and 4 carbon atoms.

and for its ionization efficiency. Then the total atomic constituency was added up. If the atomic ratios were not those of HNS, we revised our guesses and started over. This procedure was affected most by the mass 28 peak, which was much larger than any other peak. Both CO and N_2 make up its intensity, and choosing the fraction of each was the most sensitive way of controlling the total atom balance. Figure 2 represents what we feel is the best choice of mass peak assignments. It is not a unique choice, but the atom balance comes out reasonably well. The relative abundances of C, N, and H are within 5%, and the O atom abundance is short by about 25%. This shortage can be improved by changing the ratio of CO to N_2 at $M = 28$ or by letting all of the $M = 44$ be CO_2, but the abundances of both C and N atoms are adversely changed. We point out that the uncertainties in reporting the data are large, probably amounting to 50% for some of the minor constituents such as C_2H, C_3H, etc. where only one or two shots were expended to make the measurements. But a significant contribution to the uncertainty also arises from the adjustments to the ionization sensitivity of the detector. For some species, such as N_2O, C_n, this correction can be sizeable and differs widely depending on the reporting source. For other species, such as C_2H, C_3H, etc., no values are available so we make no adjustments.

Our measured HNS spectrum is more complex than the equilibrium product spectrum.[1] The stable product spectrum consists of 9

TABLE 1

Comparison of Products in Common with Equilibrium Measurements

		Fraction of Products	
Mass	Species	This Work	Equilibrium
2	H_2	0.092	0.034
16	CH_4	---	0.004
17	NH_3	<0.017	0.011
18	H_2O	0.016	0.089
27	HCN	0.026	0.004
28	N_2	0.11	0.14
	CO	0.36	0.24
44	N_2O	0.038	---
	CO_2	0.038	0.14
12-60	ΣC_n	0.123	0.33*

---

*listed as solid carbon.

species, which are listed in Table 1 with their abundances. Except for the solid carbon, we can identify almost all of these in our spectrum, but we have assigned many species that do not appear in the equilibrium products. Also, as Table 1 shows, the abundances of the common products differ considerably.

The most prominent feature of our spectrum is mass 28, to which we have assigned 80% as CO and 20% as N_2. These two products combined account for almost 50% of the product intensity. Less dramatically, in the equilibrium measurements, they account for only 38% of the products. We see much more H_2 but less H_2O than appears in the equilibrium products. There is a considerable difference between the pure carbon products in Table 1. Only about 12% of our product appears as carbon atoms or carbon clusters. At equilibrium, almost 3 times that amount eventually ends up as solid carbon or soot. As Fig. 2 shows, much of our carbon appears in many small radicals spread over the mass spectrum from mass 13 to mass 49. We may have missed some products at masses greater than M = 60 because the signals were too small. If many of these small mass peaks exist up to M = 402, a considerable amount of product could be unaccounted for in our analysis.

While many of the products that we see in HNS also appear in the spectrum we reported for PETN detonations, the details are very much different. In PETN also, there is a dominant mass peak, but it is M = 18, H_2O. This is consistent with the increased amount of hydrogen available in each explosive molecule of PETN. We observe no molecular hydrogen in the PETN products. Also, in PETN we see moderate amounts of NO_2 formed, while none is seen in HNS. Thus it appears that the nitrogen can compete more effectively for the available oxygen in PETN than it can in HNS. Probably the most important difference between HNS and PETN is the appearance of carbon clusters. Only a small mass peak of the carbon monomer is observed in PETN, but up to C_5 is easily measured in HNS.

It is not clear from Fig. 3 that we can decide what the mechanism is that is responsible for the distribution of clusters. We do not observe any intensity alternations between cluster ions containing odd and even numbers of atoms, as have been reported in some studies.[6b,c] These earlier distributions were peculiar to positive carbon cluster ions obtained by evaporation from solid carbon surfaces; odd-sized clusters with 9 atoms or less were more intense than even-sized clusters. More recent experiments employing laser ablation of carbon clusters from graphite surfaces also show evidence for intensity alternations,[6a] but these make their appearance at large cluster sizes, from 20 to 90 atoms, and only even clusters appear. Various reasons have been suggested to explain these distributions, based on stability arguments of preferred geometries. It has been suggested that small odd clusters are more energetically stable than even clusters, and that the evaporation experiments demonstrate this characteristic. In contrast, the ablation experiments have been interpreted to indicate the formation of carbyne structures in the graphite at the point where laser heating occurs which retain these basic structures into the cluster formation. Since our distributions decrease more or less monotonically with cluster size, it is clear that none of these factors invoked above play a significant part in forming the clusters we observe. For example, there is no preferential breakup of the carbon rings in stilbene leaving behind stable cluster sizes that persist through the product gases expansion.

After the detonation wave has passed through the HNS pellet, the initial expansion of the products occurs under conditions of high temperature, 3000 to 4000 K, and of high pressure, several hundred kilobar. Slower reactions are still taking place, as is evident from the fact that we see radicals that would not be present after longer, confined expansions. As the product expansion progresses, the temperature drops rapidly and carbon clusters formation can be controlled by one of two mechanisms. If the collision frequency between carbon atoms and clusters are high enough compared to the rate at which temperature drops then the cluster distribution can be reasonably close to an equilibrium distribution at the local temperature and pressure. At some point in the expansion, however, the collision frequency and the temperature become low enough that clusters grow by aggregation of carbon atoms and carbon clusters. The rate of recombination for the various cluster sizes determines the growth of the clusters, and for small clusters, the vibrational relaxation to lower lying bound states is fast compared to the recombination. Dissociative collisions become less important and the cluster size distribution departs from equilibrium.

Modeling such an expansion promises to be a sizeable undertaking. The amount of carbon in the products is large and the energy of recombination of a carbon atom to another atom or to a cluster is large,[9] amounting to 6 or 7 eV for clusters containing up to 4 atoms. Thus, the model would have to include the heat of formation added to the products, so that the equation of state of the products is complex. In Fig. 3 we have plotted an equilibrium distribution at 3400 K and a carbon pressure of 0.01 bar. It does not fit our measured distribution well, and this is about as close a fit as we found using other temperatures and pressures.[10] (Only the five species C_n, n = 1 to 5, were included in the calculation.) Thus, cluster aggregation under nonequilibrium conditions seems to be necessary to account for our measured distributions.

We cannot explain the fact that the solid Xe confined detonations changed the carbon cluster distributions so little. Evidently, carbon originating near the center of the expanding products does not form larger clusters than does carbon near the outer regions. In fact, in Fig. 3, the distribution of carbon clusters under these confined detonations seem to favor smaller clusters slightly. Higher temperatures seem to have been experienced by this material.

We have not yet determined the stage at which very large carbon clusters are formed, capable of accumulating to macroscopic soot particles. We've considered the possibility that the cluster distribution that we measure arises from dissociative ionization in our detector of much larger clusters, but this doesn't seem to be a very likely explanation. Reported fragmentation patterns from other workers[11] indicate that while our observed distributions may be altered from the true distribution, large clusters should not disappear altogether.

We did not look for ions in the detonation products. It is doubtful that ions would survive passage through small apertures over the 1 meter flight path to our detector. A special effort to detect ions near the detonation region would be necessary. Because ions can be very efficient nucleation centers[12] for cluster formation, this possibility must be examined. We also plan to look at visible and infrared absorption of light (as well as scattering light) in the expanding detonation products. Our goal is to look for other reaction intermediates than we observed in our mass spectrometer, to obtain internal molecular temperatures, and to observe the formation of macroscopic particles of soot.

REFERENCES

1) D. L. Ornellas, Calorimetric Determinations of the Heat and Products of Detonations for Explosives: October 1961 to April 1982. UCRL-52821 (1982).

2) N. C. Blais and J. J. Valentini, Proceedings VIII Symposium on Detonations, Albuquerque, New Mexico (1985) (in press).

3) C. L. Mader, "Numerical Modeling of Detonations, (Univ. of Calif. Press, D. H. Sharp and L. M. Simmons, Jr., Ed., 1979) see p. 125-131.

4) J. C. Street and A. Thomas, Fuel 34, 4 (1955).

5) A. G. Gaydon and H. G. Wolhard, Flames, Their Structure, Radiation and Temperature. (Chapman and Hall, London, 4th edition, 1979) Chap. VIII.

6) a) E. A. Rohlfing, D. M. Cox, and A. Kaldor, J. Chem. Phys. 81, 3322 (1984): b) N. Fuerstenau and H. Hillenkamp, Int. J. Mass. Spectrom. Ion Phys. 36, 135 (1981): c) R. E. Honig, J. Chem. Phys. 22, 126 (1954).

7) N. Roy Greiner and N. C. Blais, Proceedings, 17th Annual ICT Conference, Karlsruhe, FRG, 1986 (to be published).

8) A. Cornu and R. Massot, Compilation of Mass Spectral Data, 2nd edition, V1 (Heyden & Son 1975): L. J. Kieffer and G. H. Dunn, Rev. Mod. Phys. 38, 1 (1966): J. B. Mann, Recent Developments in Mass Spectroscopy, Proceedings of Int'l Conference on Mass Spectroscopy, Kyoto, 1970, (K. Ogata and

T. Hayakawa, ed.): R. T. Meyer and A. W. Lynch, High Temp. Sci. 5, 192 (1973).

9) *JANAF Thermochemical Tables*, NSRDS-NBS37 (U.S. Department of Commerce, National Bureau of Standards 2nd edition, 1971): R. T. Meyer and A. W. Lynch, High Temp. Sci. 5, 192 (1973). F. M. Wachi and D. E. Gilmartin, High Temp. Sci. 4, 423 (1972).

10) J. Lyman, private communication. The heats of formation of C_n were taken from the JANAF Thermochemical Tables.

11) K. L. Wang, *Electron Impact Ionization Cross Sections for Carbon Vapor*, Ph.D. thesis MIT, Cambridge, Massachusetts (1970).

12) R. Ball, *Flame Study of Carbon Particle Growth*, Ph.D. thesis, MIT, Cambridge, Massachusetts (1969).

This paper was prepared under the auspices of the U.S. Department of Energy.